

Determination of Pb(II) Ion with a Novel, Highly Efficient Immobilized Arsenazo III in a Polymer Matrix

Kholboeva M. B¹, Smanova Z. A², Madatov U. A², Yusupov Boburjon³, Nomozov A. K^{1,4*}, Sobirova F. A.⁵, Oybek Olimovich Daminov⁶ & Mengboyev Otabek Alijonugli⁷

¹Department of Chemical Engineering, Termez State University of Engineering and Agrotechnologies, Termez, Uzbekistan

²Faculty of Chemistry, National University of Uzbekistan, Tashkent, 100 174, Uzbekistan

³Gulistan State University, Gulistan, Uzbekistan

⁴Department of Medical and Biological Chemistry, Termez branch of Tashkent State Medical University, Termez, 1901 11 Uzbekistan

⁵Faculty of Medicine, Department of Pharmacy and Chemistry, Alfriganus University, Tashkent, Uzbekistan

⁶Internal Combustion Engines, Refrigeration and Cryogenic Technology, Tashkent State Technical University named after Islam Karimov, University Street 2, Tashkent 100 095, Uzbekistan

⁷Faculty of pedagogy and social-humanitarian sciences, Foreign languages, Termez university of economics and service, Termez, 1901 11, Uzbekistan

Received 21 April 2025; revised 22 January 2026; accepted 09 March 2026

In this study, a novel analytical reagent based on arsenazo III immobilized on a polymer matrix composed of polyacrylonitrile, polyethylene polyamine, and dichloroethane (PPD) was developed and applied for the spectrophotometric determination of Pb(II) ions. The proposed method demonstrated standard analytical and metrological characteristics for the highly accurate determination of Pb(II) ions, as evidenced by a relative standard deviation (Sr) of 0.06 and a minimum detectable concentration (C_{\min}) of 0.24 $\mu\text{g/L}$. The accuracy and reproducibility of the method were evaluated using Student's *t*-test and Fisher's F-test. Comparison of the experimental and tabulated values (experiment = 1.09; $t_{\text{table}} = 2.83$, $F_{\text{experiment}} = 2.52$; $F_{\text{table}} = 4.47$) confirmed the reliability of the proposed analytical procedure. At pH 5.8 in an acetate buffer medium, the Pb(II)–arsenazo III complex immobilized on the PPD matrix exhibited a maximum analytical signal at a wavelength of 640 nm. The measurement results followed the Beer–Lambert–Bouguer law, showing a linear relationship in the Pb(II) concentration range of 0.04–2.4 $\mu\text{g/mL}$. The method is simple, rapid, cost-effective, and allows direct ion determination in water samples with high sensitivity and selectivity.

Keywords: Direct ion determination, Sorption spectrophotometry, Lead detection, Polymer matrix, Water sample

Introduction

Lead (Pb) is one of the most commonly detected heavy metals in contaminated water sources, frequently exceeding the World Health Organization (WHO) guideline of 10 $\mu\text{g/L}$, which poses severe ecological and health risks.^{1,2} Recent studies have focused on developing highly selective and sensitive methods for Pb(II) detection.^{3,4} Liss López *et al.* used three functional monomers—acrylic acid (ACRY), 2-acrylamido-2-methylpropane sulfonic acid (AMPSA), and allylamine (ALLY)—for the design of ion-imprinted polymers (IIPs). Adsorption studies under optimized conditions demonstrated that IIP-AMPSA exhibited the highest Pb²⁺ adsorption capacity (51.84 mg/g), outperforming

IIP-ACRY (31.02 mg/g) and IIP-ALLY (12.90 mg/g), consistent with the computational predictions.^{5,6} Ashirova *et al.* studied sulfarsazen (SFN) immobilization on polyethylene polyamine-modified polyacrylonitrile (PPA) analytical matrix for Hg(II) determination. Optimal analytical conditions were observed at pH 9.8 and 520 nm, with a linear range of 2–42 mg/L, a detection limit of 0.4 mg/L, and an adsorption efficiency of ~98%. SFN/PPA matrix demonstrated strong selectivity even in the presence of common interfering ions (Ca^{2+} , Sr^{2+} , Ba^{2+} , Mg^{2+} , Na^+ , Cl^- , I^-), enabling accurate Hg(II) determination in wastewater samples.^{7–10} Recent studies on polymer-based nanocomposites have demonstrated that incorporation of inorganic dopants, such as vanadium pentoxide into poly (O-toluidine), significantly alters both dielectric behaviour and electrical conductivity,

* Author for Correspondence
E-mail: abornomozov055@gmail.com

highlighting the potential of such systems for advanced material applications.¹¹ Poly(O-toluidine) (POT)-ZnO nanocomposites have been developed via in situ chemical polymerization to enhance structural, thermal, and electrical properties, also improved crystallinity, uniform filler distribution, and higher thermal stability with increasing ZnO content. Results shows that the 75 wt% composite (PZnO75) exhibits the highest performance, making it a promising material for energy storage and electronic applications.¹²

The aim of the current work is to immobilize arsenazole III on a fibrous sorbent and develop a new economical, rapid sorption-spectrophotometric method for the determination of lead ions using immobilized arsenazole III and its application in the determination of Pb(II) ion in natural objects.

Materials and Methods

Materials

All chemicals used in this study, including polyacrylonitrile, polyethylene polyamine, arsenazo III(3,6-bis-[(2-arsonophenyl)azo]-4,5-dihydroxy-2,7-naphthalenedisulfonic acid) and 1,2-dichloroethane, Pb(CH₃COO)₂·3H₂O salt were obtained from Sigma-Aldrich MilliporeSigma (Merck Group) and Ximreaktivinvest LLC, and were used without further purification.

Methods

In order to determine the reaction mechanisms of the immobilized compounds, as well as the resulting complex formation, infrared (IR) spectra were recorded on a Bruker Fourier spectrometer (Invenio S-2021, in the range of 4000–400 cm⁻¹).

During the research, a pH meter called "BANTE pH meter-210" was used to measure the optimal environments of solutions.

In the solution medium, optical densities and wavelengths of the reagent and complex were measured by absorption spectroscopy using an EMC-30PC-UV spectrophotometer. In the sorption determination, the optimal conditions for complex formation were found using an X-Rite Eye One Pro mini spectrophotometer.

Experimental Part

In this research work, a 0.02% solution of the organic reagent 3,6-bis-[(2-arsonophenyl)azo]-4,5-dihydroxy-2,7-naphthalenedisulfonic acid (C₂₂H₁₈As₂N₄O₁₄S₂, Mr = 776.37 g/mol) was prepared as a reagent for the determination of lead (II) ion. To

prepare a standard 1·10⁻⁴ M solution of Pb (CH₃COO)₂·3H₂O salt, 0.0325 g of dry salt was weighed into a 200 ml volumetric flask using an analytical balance with an accuracy of 0.0001 and dissolved with distilled water to the mark of the flask. Structure of the analytical reagent is given in scheme 1.

Buffer solutions

Acetate buffer solution was used to provide the medium for the solutions. To prepare a pH = 5.5 solution, 100 ml of 1N CH₃COOH and 50 ml of 1N NaOH were added to 500 ml flasks, and to prepare a pH = 5.8 solution, 79.5 ml of CH₃COOH and 50 ml of NaOH were added and made up to the mark with distilled water.

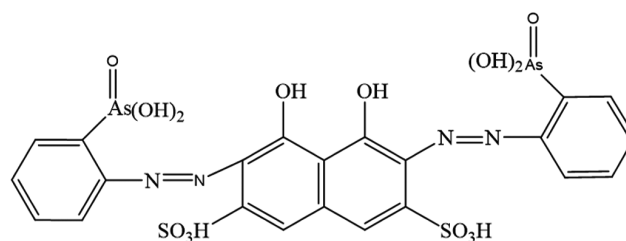
Selection of Polymer Carrier Sorbent

For lead salt and Arsenazo III reagent, PPD sorbent was used, which is obtained by sequentially chemically modifying polyacrylonitrile in the presence of polyethylenepolyamine and dichloroethane. The synthesis reaction of the sorbent is shown in scheme 2 below:

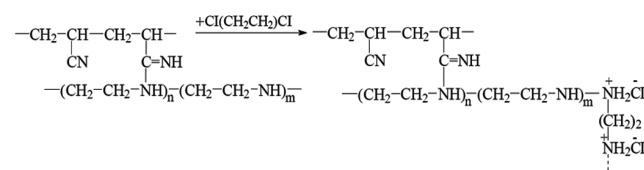
In this study, PPD fiber was used as the carrier sorbent, and 0.2 g was taken and exposed to a standard solution of 0.1 molar HCl hydrochloric acid for 24 hours to activate the sorbent and neutralized with distilled water.

Immobilization Process into a Polymer Matrix

The mechanism of immobilization of the selected arsenazo III analytical reagent on polymer supports is presented below. First step. PPD polymer was activated in 0.1 N hydrochloric acid (~R-NH₃⁺Cl⁻). In

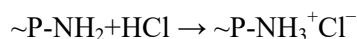


Scheme 1 — Molecular structure of the analytical reagent (3,6-bis-[(2-arsonophenyl)azo]-4,5-dihydroxy-2,7-naphthalenedisulfonic acid)

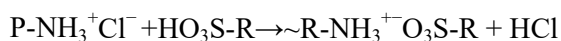


Scheme 2 — Synthesis of (arsenazo III reagent and PPD) sorbent

this process, 0.2 g of polymer support was placed in a 25 ml flask, then 10 ml (0.1 N) HCl solution was added and the resulting solution was activated at room temperature for 1 day. Then the support matrix was washed with distilled water to a neutral state (pH = 7). As a result, $\sim\text{R-NH}_3^+\text{Cl}^-$ was formed.



The second step is to obtain an immobilized form of the carrier polymer using the Arsenazo-3 analytical reagent. In this process, 10.0 ml of a 2.57×10^{-4} M or 0.02% Arsenazo-3 solution and 0.2 g of the ionic forms of the carrier polymers ($\sim\text{P-NH}_3^+\text{Cl}^-$) are added to a 25.0 ml flask, after which the mixture is stirred for 9–10 minutes. Then, the carrier matrix immobilized with Arsenazo-3 ($\sim\text{R-NH}_3^+\text{-O}_3\text{S-R}$) is washed with distilled water and then dried at room temperature. During this immobilization process, the sulfo functional groups of the Arsenazo-3 analytical reagent form bonds with the amino functional groups of the sorbents as a result of electrostatic interaction.



Third stage is the process of complexing the lead ion with the arsenazo III ion chemically sorbed to the polymer matrix in a static process. The reaction of lead (II) with the arsenazo III reagent in $\sim\text{R-NH}_3^+\text{-O}_3\text{S-R}$ was carried out as follows: a 1×10^{-4} M standard solution of lead (II) was mixed with the immobilized carrier polymer ($\sim\text{R-NH}_3^+\text{-O}_3\text{S-R}$) in a flask; as a result, $\sim\text{R-NH}_3^+\text{-O}_3\text{S-R-Pb}$ was formed. Pb (II) ions are strongly bound to the hydroxyl functional groups through an ionic bond and to the $-\text{N}=\text{O}$ functional group through a coordination bond.^{13,14}

Results and Discussion

Quantum Chemical Calculation

Electrostatic potential surfaces are important in identifying the reaction centers of molecules, especially in noncovalent interactions. These surfaces indicate the nucleophilic and electrophilic centers of molecules. In Figs 1a and 1b, the red dots represent regions with a high electron cloud density and a negative electrostatic potential, i.e., regions with more electrons. The purple centers represent regions with a positive potential and fewer electrons.¹⁵

Electrostatic Potential: In the electrostatic potential (ESP) surface of Arsenazo III (Fig. 1), red regions indicate potential minima, while purple regions indicate potential maxima. Both large maxima and small minima are observed in the figure. Additionally, white spheres represent minima, and red spheres represent maxima. The electrostatic potential analysis revealed that the coupling reactions occur primarily through the $-\text{OH}$ and $-\text{N}=\text{O}$ functional groups.

It was found that the highest electron cloud density of the arsenazo III reagent is 0.758, which belongs to the SO_3H group. Therefore, it can be assumed that the immobilization of the arsenazo III reagent on the fibers occurs through the sulfo (SO_3H) group of the reagent (Fig. 1b).

HOMO-LUMO: In computational chemistry, HOMO (Highest occupied molecular orbital) and LUMO (Lowest unoccupied molecular orbital) are key concepts in analyzing the electronic structure of a molecule. They describe the highest occupied and lowest unoccupied orbitals in a molecule.

HOMO-LUMO energy gap: The energy difference between HOMO and LUMO is important in determining the reactivity and stability of a molecule. This difference is also called the energy gap. A small HOMO-LUMO

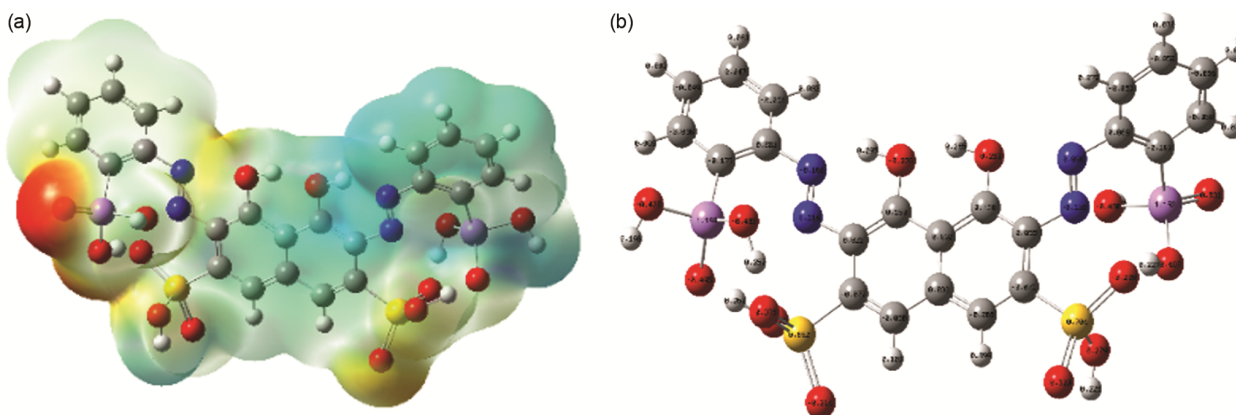


Fig. 1 — Arsenazo III: (a) Electrostatic potential surface, (b) Electron cloud density

gap makes a molecule reactive towards chemical reactions, while a large gap increases stability. These aspects could be seen from Fig. 2.

1. Reactivity:

1. If it is between 0–2 equiv, it reacts easily and quickly
2. If it is between 2–4 equiv, it reacts under certain conditions
3. If it is greater than 4 equiv, it is inert
4. Soft if it is less than 1 equiv, hard if it is greater than 1 equiv

$$E_L = -0.12387 \text{ eV} \quad E_H = -0.24506 \text{ eV}$$

$$\Delta E = E_L - E_H = -0.12387 - (-0.24506) = 0.12119 \text{ eV}$$

Conclusion: the substance reacts easily and the substance is soft.

Spectrophotometric Analysis

The EMC-30PC-UV-1800 spectrophotometer was used to measure the maximum absorption area of the arsenazo III reagent. The measurements were taken against the reference solution arsenazo III and the absorption areas were compared. The maximum

absorption wavelength of the arsenazo (III) reagent was observed at 540 nm. This information was important for determining the maximum absorption wavelengths of the reagents, and the analysis for subsequent experiments was based on changes in these wavelengths.¹⁶

Optimal Carrier

To select the optimal carrier, 0.2 g of several types of sorbents were weighed on an analytical balance with an accuracy of 0.0001 and processed using a 0.1 N HCl standard solution, and then the matrices were washed, dried, and stored in special petri dishes. The carriers were placed in a glass, and 0.02% solutions of the selected organic reagent arsenazo III were added to them. Then the optical density of the solutions before and after immobilization was measured on an “EMC-30PC-UV, UV-5100 UV VIS” spectrophotometer, and after immobilizing the selected activated carrier organic reagent under optimal conditions, their spectra were measured on an X. Rite Eye-one-pro reflectance spectrophotometer, calibrated against the original polymer matrices based on the BaSO₄ matrix, and the results are presented in Fig 3.⁽¹⁷⁾

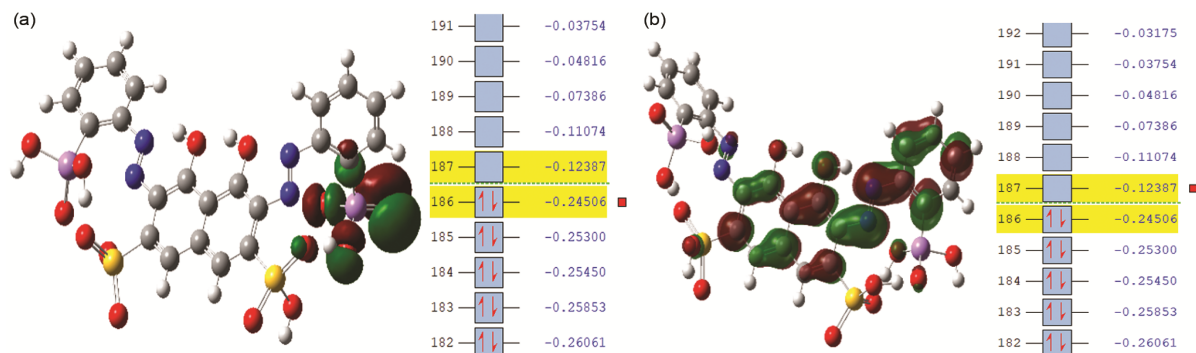


Fig. 2 — Molecular orbital of arsenazo III: (a) The HOMO (highest occupied molecular orbital), (b) The LUMO (the lowest unoccupied molecular orbital)

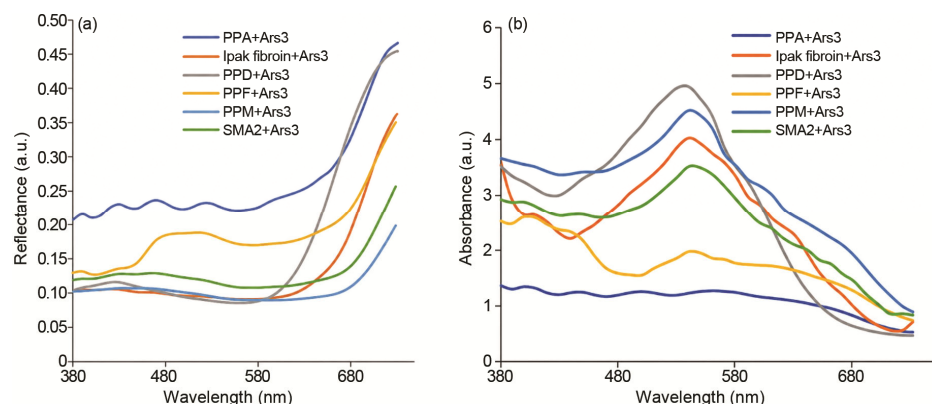


Fig. 3 — Arsenazo III reagent immobilized on several types of sorbents: (a) light reflectance spectra; (b) Kubelka–Munk function representation of the reflectance spectra

The reflectance spectra of the best immobilized organic reagents on the sorbents were measured and analyzed on an X-rite eye-one Promini Spectrophotometer. The results are presented in Fig. 3.

In the above results, it was observed that the organic reagent Arsenazo III was the best carrier to PPD fiber and they were selected as the sorbent.¹⁸⁻²¹

Time Dependence of Reagent Immobilization

To study the time dependence of immobilization of the Arsenazo III reagent on PPD fiber, the fiber was incubated in a 1×10^{-3} M solution of the reagents for 1–50 minutes and the analytical signals were measured, the results obtained are presented in Fig. 4.

It can be seen from the graph above that 15 minutes is sufficient for complete immobilization of the Arsenazo III reagent.

The Dependence of Complex Formation on the pH of the Medium and the Nature of the Buffer

In a 25 ml standard volumetric flask, 2 ml of 0.001% aqueous solution of ARSENAZO III reagents, 5.0 ml of a buffer solution of known pH and 1 ml of Pb²⁺ solutions (60 µg/ml) were added and double distilled water was added to the mark of the flask. The pH of the resulting solutions was redetermined using a PHS-3E pH meter (China) and the optical densities ($\lambda_{max} = 540, l = 1.0$ cm) were

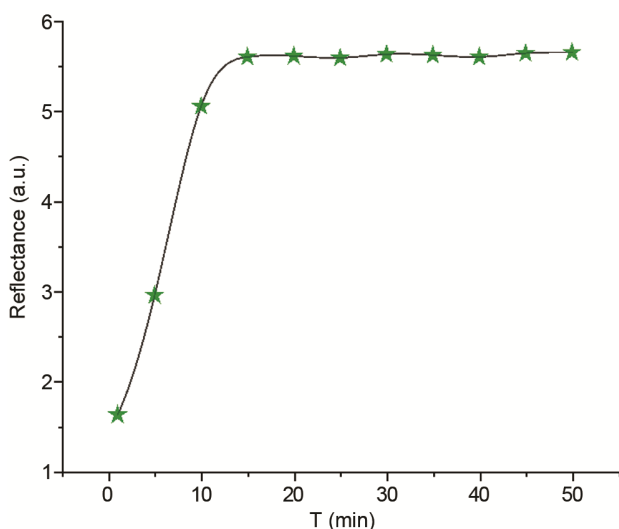


Fig. 4 — Time dependence of reagent immobilization

measured relative to standard reference solutions. The results obtained are presented in Fig. 5 and Table 1.

From Fig. 5(d) and Table 1, it can be concluded that the complex formation with immobilized ARSENAZO III and Pb²⁺ ions leads to the formation of a stable complex between pH = 5–6. The highest analytical signal was observed at pH = 5.8. For the subsequent analysis processes, the acetate buffer solution was used at pH(Pb²⁺) = 5.8 for the formation of lead complexes.²²⁻²⁴

Observance of the Bouguer-Lambert-Beer law

Experiments were conducted to study the obedience of the Bouguer-Lambert-Beer law in the determination of lead (II) ions using immobilized arsenazo III salt reagents.

The applicability of the Beer–Lambert–Bouguer law for Pb(II) ion concentrations in a 25 mL solution within the range of 1–60.0 µg/mL is demonstrated in Fig. 6. A deviation from linearity is observed at higher concentrations; however, the method remains sufficiently sensitive for the detection of metal ions in environmental samples.

Spectral Characterization of the Complex Formation of Lead(II) ion with Immobilized Arsenazo III

The complex of Arsenazo III immobilized with PPD sorbent, reagent immobilized on the sorbent and Pb (II) ions was analyzed by the absorption spectrophotometric method. As can be seen from the analysis results (Table 2), the absorption spectrophotometric analysis of the Arsenazo III reagent and its complex with lead (II) ions in solution showed that the reagent absorbs at a wavelength of

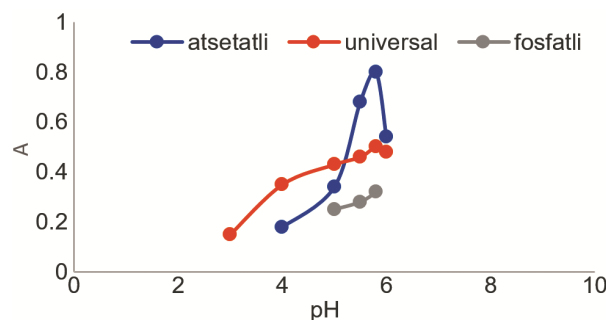


Fig. 5 — Dependence of complex formation on the environment

Table 1 — Selection of optimal buffer solution

R+Me	Buffer solution	pH									
		2	3	4	5	5.5	5.8	6	7	8	9
Arsenazo III+Pb ²⁺	Acetate (A)	—	—	0.18	0.35	0.68	0.8	0.54	—	—	—
	Universal(A)	—	0.15	0.35	0.43	0.46	0.5	0.48	—	—	—
	Phosphate(A)	—	—	—	0.25	0.28	0.32	—	—	—	—

Table 2 — Spectral characterization of the complex formed between Pb(II) ions and the Arsenazo III reagent was performed under the following conditions: path length = 1.0 cm, and Pb²⁺ concentration = 60 µg.

Complex color, phase	pH	λ, HR nm	λ, MeR nm	Δλ	C _{Pb} ²⁺ mkg/ml
Purple, solution	5-6	540	610	70	60
Purple, solid	5-6	540	610	70	60

Note: HR -reagent, MeR-metall-reagent complex

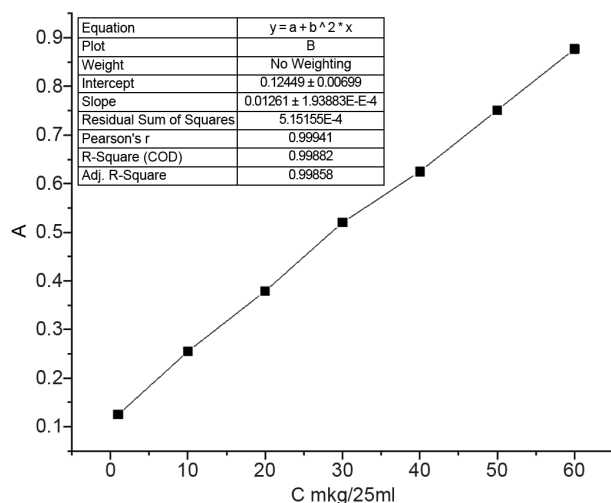


Fig. 6 — Graph showing the dependence of optical density on the amount of Pb(II) ions added

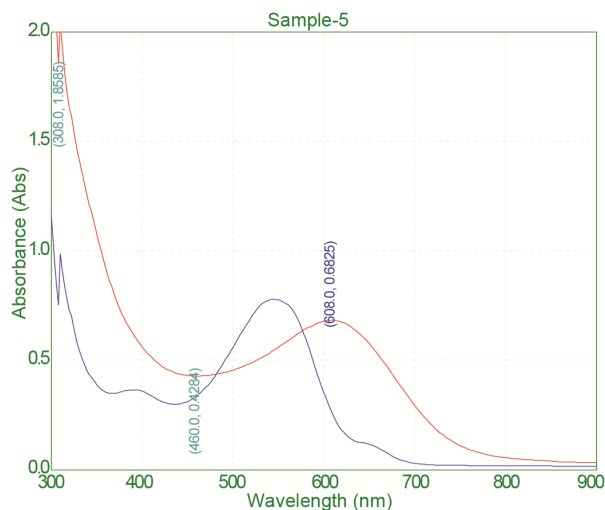


Fig. 7 — Absorption spectra of ARSENAZO III ($\lambda_p = 540$ nm) and its complex with lead (II) ion in solution ($\lambda_k = 610$)

540 nm, and its complex with lead ions at 610 nm (Fig. 7), with a contrast of 70 nm. When analyzed by the absorption spectrometer for the immobilized reagent and the complex with lead ions (Figs 8 and 9), the values of the maximum analytical signal were observed at 540 nm and 610 nm, respectively, which indicates that the analysis was carried out correctly.^{25,26}

The increase in reaction contrast on the solid substrate indicates that the immobilized reagent adopts a more rigid structure due to steric hindrance. As rotational and vibrational motions are restricted, the analytical signal reaches its maximum during immobilization.

IR Spectrum Analysis

The structure of the complex formed by lead (III) and the arsenazo III reagent immobilized on the polymer matrix and the mechanism of immobilization of the reagent on the fiber were determined using IR spectrometry. The infrared spectra of the complex were studied in the frequency range of 4000-400 cm⁻¹ using an IR-Fourier-spectrometer “Bruker Invenio S-2021”. To study the mechanism of immobilization of the arsenazo III reagent on the fiber, the IR spectra of the complex formed with the fiber, the reagent, and the metal ion of the immobilized reagent were measured and are presented in Fig. 9.^(27,28)

In the IR spectrum of Arsenazo III, we can observe an absorption line formed by the valence vibrations of the -OH bond in the 3369 cm⁻¹ region, absorption lines formed by the valence vibrations of the -C-H (sp³) bond in the 2916 cm⁻¹ region, absorption lines formed by the valence vibrations of the =C-H (sp²) bond in the 3081 cm⁻¹ region, an absorption peak of the -C-N=N bond in the 1620 cm⁻¹ region, absorption lines belonging to the -SO₂ in the 1413-1478 cm⁻¹ region, absorption lines belonging to the C-O-H bond in the 1169-1297 cm⁻¹ region, absorption lines belonging to the -C-S- bond in the 785 cm⁻¹ region, and absorption lines formed by the vibrations of the As-O bond in the 423-626 cm⁻¹ region.³⁰

The broadening of the absorption peaks in the IR spectrum of PPD fiber immobilized with Arsenazo III reagent in the 3342 cm⁻¹ region due to the vibrations of the -O-H bond and the 3273 cm⁻¹ region due to the formation of hydrogen bonds and donor-acceptor bonds in this region indicates that the reagent is attached to the fiber. Because these peaks occur separately in the IR spectrum of the starting materials. We see that the peaks in the 478-909 cm⁻¹ region are significantly broadened compared to the IR spectrum

Table 3 — FTIR Spectral Analysis of PPD Fiber, Immobilized Arsenazo III, and the Pb(II)–Immobilized Arsenazo III Complex

Compound	$\nu =$ SO ₂ OR	$\nu =$ C=N va (C- N)	$\nu =$ O- As	$\nu =$ OH	$\nu =$ C-H (Ar)	$\nu =$ O- Pb	$\nu =$ C-H (sp ³)	$\nu =$ CN	$\nu =$ N-H
PPD	—	1646	—	—	—	—	2852– 2923	2242	3185
Immobilized (Arsenazo III)	1453	1654	478	3342	3042	—	2926– 2853	2192	3273
Immobilized arsenazo III Pb(II) complex	1455	1647	—	3373	2923	502	2852	2242	—

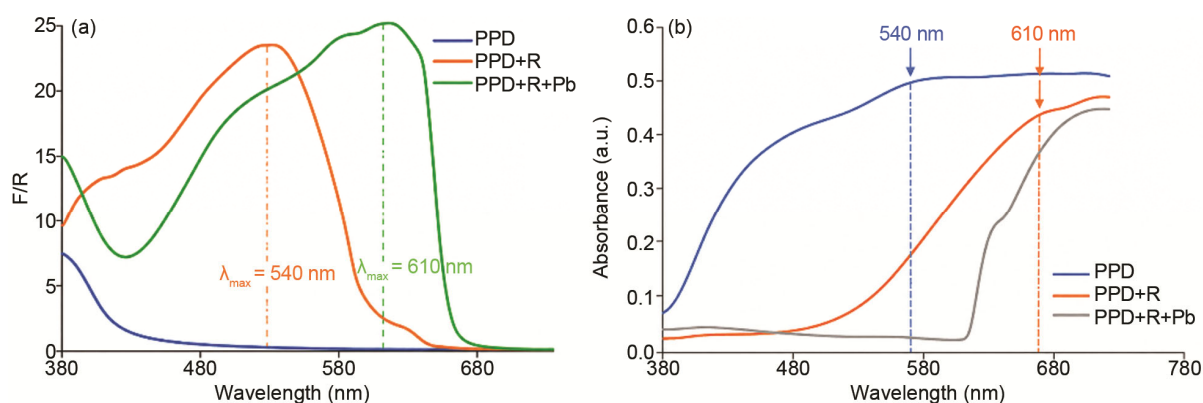


Fig. 8 — The light reflection spectrum of the carrier sorbent PPD, Arsenazo III immobilized on it, and the complex: (a) the spectrum, (b) the Kubelka-Munk function

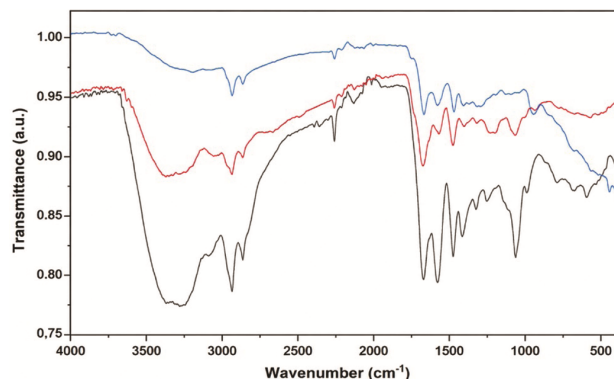


Fig 9 — IR spectrum of the complex of immobilized arsenazo III with Pb(II) ion immobilized on it, and the complex.

of the starting products, which indicates an increase in intermolecular and intramolecular hydrogen bonds in the product structure. The formation of absorption lines in the 478–499 cm⁻¹ region due to the vibrations of the As-O bond, which are not found in the IR spectrum of the fiber, also indicates the immobilization of Arsenazo III on the fiber. In the IR spectrum of the immobilized arsenazo III complex with Pb (II) ion, we can see that the main changes are observed in the 502 cm⁻¹ and 554 cm⁻¹ regions, while

the absorption lines belonging to the main functional groups are preserved.³¹ In particular, we can observe that absorption lines belonging to the -O-Pb- and -N-Pb- bonds are formed in these regions Table 3.

X-ray Fluorescence Analysis of the Complex

The X-ray fluorescence (XRF) spectrum of Arsenazo III immobilized on the PPD sorbent exhibits characteristic peaks of arsenic, which are absent in the spectrum of the bare sorbent. The XRF spectrum of the Pb(II)–immobilized Arsenazo III complex shows prominent Pb peaks, confirming the interaction between the immobilized reagent and lead ions (Fig. 10).

SEM Analysis

SEM analysis of immobilized arsenazo III and its complex with Pb (II) ion. Morphological studies and elemental composition of fibers were carried out using a scanning electron microscope "VO-MA 15" (Zeiss, Germany). To obtain information about the composition of elements, electron photographs with selected locations, composition tables and graphic spectra of fiber samples, immobilized arsenazo III and

Analyzed result

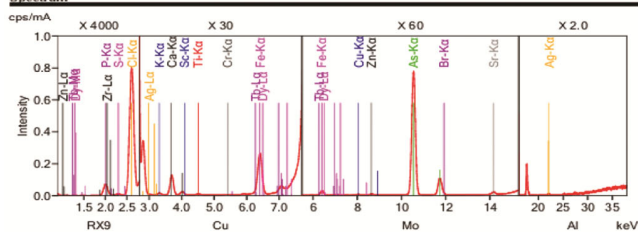
Sample Information

Sample name M. PPD tola Arsen. (III)
 File name M. PPD tola Arsen. (III)
 Application Umumiy.
 Date 2024/ 2/23 10:03
 Analyzed by
 Counts 1
 Comment

Analyzed result(FP method, Scatter)

No.	Component	Result	Unit	Stat. Err.	LLD	LLQ
1	Cl	14.6	mass%	0.0093	0.0054	0.0161
2	Br	<0.0001	mass%	0.0001	0.0001	0.0004
3	P	4.26	mass%	0.0090	0.0038	0.0115
4	S	0.375	mass%	0.0036	0.0089	0.0266
5	K	0.0296	mass%	0.0017	0.0027	0.0080
6	Ca	0.164	mass%	0.0027	0.0011	0.0033
7	Ti	0.0044	mass%	0.0003	0.0006	0.0019
8	Cr	0.0010	mass%	0.0001	0.0003	0.0008
9	Fe	0.0248	mass%	0.0006	0.0006	0.0019
10	Cu	0.0031	mass%	0.0001	0.0001	0.0004
11	Zn	0.0028	mass%	<0.0001	0.0001	0.0003
12	As	0.0879	mass%	0.0003	0.0002	0.0006
13	Sr	0.0012	mass%	<0.0001	<0.0001	0.0001
14	Zr	0.0084	mass%	0.0009	0.0002	0.0006
15	Ag	0.0006	mass%	<0.0001	<0.0001	0.0003
16	Tb	0.0071	mass%	0.0008	0.0018	0.0054
17	Dy	0.0044	mass%	0.0005	0.0011	0.0033

Spectrum



Analyzed result

Sample Information

Sample name M. PPD tola Arsen. (III) Pb
 File name M. PPD tola Arsen. (III) Pb
 Application Umumiy.
 Date 2024/ 2/23 10:14
 Analyzed by
 Counts 1
 Comment

Analyzed result(FP method, Scatter)

No.	Component	Result	Unit	Stat. Err.	LLD	LLQ
1	Cl	1.72	mass%	0.0019	0.0012	0.0037
2	Mg	0.780	mass%	0.0207	0.0445	0.133
3	Si	0.329	mass%	0.0034	0.0064	0.0191
4	P	1.83	mass%	0.0040	0.0045	0.0135
5	S	3.23	mass%	0.0053	0.0119	0.0358
6	Ca	0.0442	mass%	0.0013	0.0014	0.0041
7	Ti	0.0024	mass%	0.0003	0.0005	0.0016
8	Cr	0.0007	mass%	<0.0001	0.0002	0.0006
9	Fe	0.0138	mass%	0.0004	0.0008	0.0025
10	Ca	0.0226	mass%	0.0006	0.0015	0.0046
11	Ge	0.0025	mass%	0.0001	0.0003	0.0010
12	As	0.216	mass%	0.0011	0.0040	0.0121
13	Se	0.0026	mass%	0.0002	0.0005	0.0014
14	Zr	0.103	mass%	0.0011	0.0004	0.0011
15	Re	0.0113	mass%	0.0004	0.0007	0.0021
16	Ir	0.0862	mass%	0.0013	0.0035	0.0104
17	Pb	2.59	mass%	0.0032	0.0045	0.0135
18	At	0.0035	mass%	0.0003	0.0007	0.0021
19	Tb	(0.0051)	mass%	0.0009	0.0024	0.0071
20	Dy	(0.0046)	mass%	0.0007	0.0019	0.0058

Spectrum

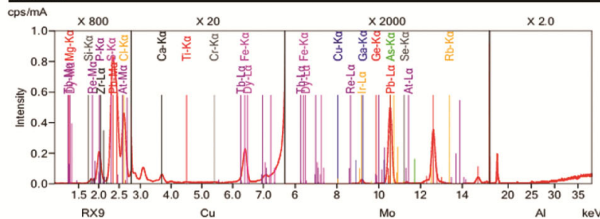


Fig 10 — (a) XRF spectrum of the Pb(II)-immobilized Arsenazo III complex, showing prominent Pb peaks; (b) confirmation of the interaction between the immobilized reagent and Pb(II) ions

its complex with lead ions were presented. The reagent immobilized on the fiber in an appropriate medium was immersed in the studied lead solution, prepared for analysis and after 15 minutes was removed and examined under a scanning electron microscope.³² The results are presented in Figs 11 & 12.

When the PPD fiber matrix with the arsenazo III reagent immobilized was analyzed using a scanning electron microscope, it can be seen from the spectrum (Figs 12a, 12b, 12c) and table that the chlorine in the carrier was replaced by arsenazo III, since the spectra corresponding to arsenic atoms were clearly visible. Then, SEM analysis of the complex formed with Pb showed that the percentage concentration of N and O atoms decreased and a signal corresponding to Pb was formed.³³⁻³⁶

The SEM-EDX analysis of the immobilized 3,6-bis-[(2-arsenophenyl)azo]-4,5-dihydroxy-2,7-naphthalenedisulfonic acid shows intense peaks corresponding to C (49.04 ± 0.03; 54.73 ± 0.04), N (24.91 ± 0.09; 23.84 ± 0.08), O (25.32 ± 0.07; 21.22 ± 0.06), S (0.35 ± 0.00; 0.15 ± 0.00), and As (0.38 ± 0.02; 0.07 ± 0.00), while elements with very low probability appear only as minor lines. In the solid-phase Pb²⁺ complex, the decrease in N and O concentrations from the original SEM data, along with the appearance of an intense Pb peak, confirms the successful formation of the complex in the solid state.

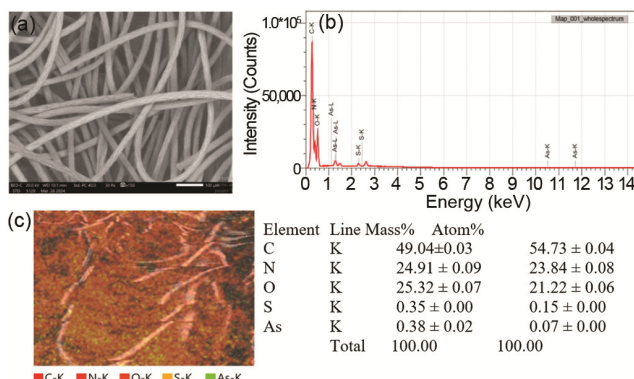


Fig. 11 — Arsenazo III immobilized on PPD fiber: (a) SEM image, (b) SEM spectrum, (c) Morphological study

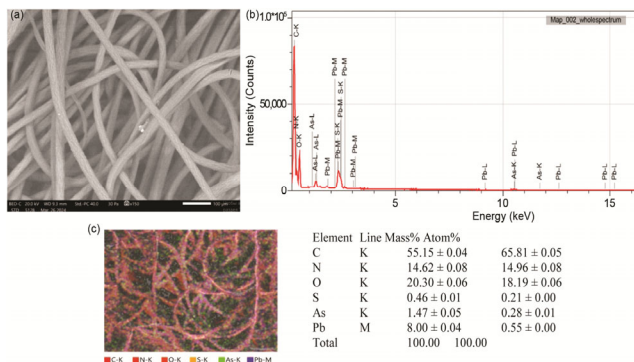
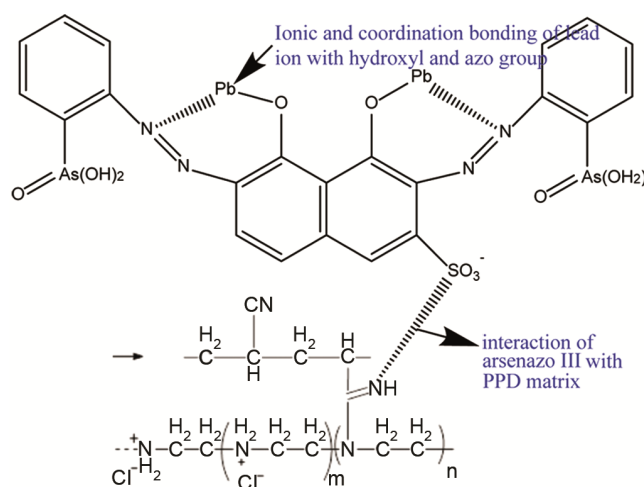


Fig. 12 — Complex of arsenazo III reagent immobilized on PPD with lead (II): (a) SEM image, (b) SEM spectrum, (c) Morphological study

As can be seen from the obtained X-ray fluorescence and SEM results, it can be concluded that arsenazo was immobilized on the PPD fiber, and the Pb (II) ion interacted with the immobilized organic reagent. This indicates the correctness of the developed sorption-spectrophotometric method. Structure of the complex formed by Pb(II) ion with arsenazo III in a solid matrix is given below in scheme 3.

The sensitivity index of the developed method according to Sendel was found to be $0.001 \mu\text{g}/\text{cm}^2$, with light absorption as follows:

$$S. b. s. = \frac{60 \times 1.0 \times 0.001}{0.7 \times 25} = 0.00342 \frac{\text{mkg}}{\text{sm}^2}$$



Scheme 3 — probable structure of the complex formed by Pb(II) ion with arsenazo III in a solid matrix

The results of the analysis were summarized and presented in the Table 4.

Application of the Developed Sorption-Spectrophotometric Method for the Determination of Pb (II) to the Analysis of Complex Model Mixtures

To apply the developed method to the analysis of real objects, a complex model mixture close to the composition of the natural object was initially prepared, and the sorption-spectrophotometric determination of Pb (II) ion in this solution was carried out using the same method and conditions as for individual solutions. The analysis results are presented in Table 5.

Competitiveness Assessment of the Sorption-Spectrophotometric Method for the Determination of Pb (II) ion

To assess the competitiveness of the proposed sorption-spectrophotometric method for the determination of Pb (II) ion, as well as to determine the reliability of the results obtained, some metrological and analytical parameters of other alternative methods were compared. The results are presented in Table 6.

The data in Table 7 demonstrate the accuracy of the developed method, and its comparison with other independent methods shows that the proposed methods are in no way inferior to existing and widely used methods in chemical analysis for some metrological characteristics. Thus, the developed method can be used in the analysis of technical and real objects.³⁴⁻³⁷

According to ompares the performance of the Sorption-Spectrophotometric (SSF) and Inversion-

Table 4 — Comparison of optimal conditions for complexation of Pb(II) with Arsenazo III in solution and on a PPD polymer carrier

Parameters	Conditions for the formation of the complex	
	In solution	PPD in a polymer matrix
λ (nm)	610	610
Optimal pH	5.8	5.8
Lower detection limit mkg/ml	0.04	0.04
Time to manifestation of complex formation (min)	15	7–10
Selectivity	Co(100), Ni(50), Cu(50), Al(100), Zr(10), Mo(10), W(50), Cd(100)	Co(100), Ni(50), Cu(50), Al(100), Zr(10), Mo(10), W(50), Cd(100)

Table 5 — Results of the determination of Pb(II) ion in artificial mixtures with immobilized arsenazo III ($P = 0.95$ $n = 5$)

Composition of the mixture being analyzed, μg	Found Me, mkg ($P = 0.95$; $n = 5$)		
	$-\bar{x} \pm \Delta X$	S	S_r
Pb(2.0) + Fe(5.0) + Zn(15)	1.99 ± 0.02	0.017	0.008
Pb(1.0) + Cr(10.0) + Cd(13.0) + Cu(10.0)	0.99 ± 0.03	0.025	0.026
Pb(3.0) + Mn(5.0) + Fe(15.0) + Mn(10.0)	2.98 ± 0.02	0.021	0.007
Pb(5) + Ca(3.0) + Mg(2.0) + Cu(10.0) + Fe(30.0)	4.98 ± 0.02	0.02	0.004

Table 6 — Results of competitiveness assessment by comparison with data obtained using other independent methods for the determination of Pb (II) ion in natural waters (n = 5; P = 95).

Sample No	Developed method		Spectrophotometry		Inversion voltammetry	
	$-x \pm \Delta X$	S_r	$-x \pm \Delta X$	S_r	$-x \pm \Delta X$	S_r
1	4.99 ± 0.02	0.004	4.97 ± 0.04	$\frac{0.07}{0.07}$	4.97 ± 0.03	0.006
2	9.97 ± 0.05	0.005	10.03 ± 0.18	$\frac{0.016}{0.16}$	9.96 ± 0.06	0.072
3	14.97 ± 0.04	0.002	14.96 ± 0.003	$\frac{0.003}{0.03}$	14.97 ± 0.026	0.002

Table 7 — Comparison of the competitiveness of the sorption-spectrophotometric method and the inversion-voltammeterometric method for the determination of Pb (II) ion in technogenic waters (n = 11; $f_1 = f_2 = 11$ P = 0.99)

Object analysis	SSF method		IV method	
	Sample, $\mu\text{g/ml}$	S_r	Sample, $\mu\text{g/ml}$	S_r
Technogenic water	0.4	0.07	0.4	0.05
t- criteria	$T_{\text{calc.}} = 1.65; t_{\text{table}} = 3.17$		$t_{\text{calc.}} < t_{\text{table}}$	
F- criteria	$F_{\text{calc.}} = 1.5; F_{\text{table}} = 4.46$		$F_{\text{calc.}} < F_{\text{table}}$	

Voltammeterometric (IV) methods for the determination of Pb(II) in technogenic waters (n = 11; $f_1 = f_2 = 11$, P = 0.99). Both methods yielded identical mean Pb(II) concentrations of 0.4 $\mu\text{g/mL}$, indicating that either technique can reliably quantify lead in these complex water matrices. The standard deviation was slightly higher for the SSF method ($S_r = 0.07 \mu\text{g/mL}$) compared to the IV method ($S_r = 0.05 \mu\text{g/mL}$), suggesting marginally lower precision for SSF; however, this difference was not statistically significant. These findings indicate that the SSF method is not only competitive with the IV method in terms of accuracy but also offers the advantages of simplicity, lower cost, and potential applicability for rapid in-field analysis. Furthermore, the robustness of the SSF method in handling technogenic water samples with potentially interfering matrix components underscores its suitability as an alternative analytical technique for routine monitoring of Pb(II) contamination.

To assess the accuracy of the developed method, we checked it with tabular data using Student's coefficient and Fisher's criteria, and we observed that the obtained analysis results were correct.

Conclusions

This study presents the development and validation of a novel sorption-spectrophotometric methodology for the quantitative determination of Pb(II) ions using Arsenazo III immobilized on a PPD polymeric matrix. The method exhibited high analytical performance, with a detection limit of 0.04 $\mu\text{g/mL}$, a relative standard deviation of 0.06, and linear response in the 0.04–2.4 $\mu\text{g/mL}$ range, consistent with the Beer–Lambert–Bouguer law. Spectroscopic, IR, XRF, and

SEM analyses confirmed efficient immobilization of the reagent and robust formation of the Pb(II)–Arsenazo III complex. The approach demonstrated excellent selectivity against multiple potentially interfering metal ions, while statistical evaluation using Student's t-test and Fisher's F-test verified its reliability and reproducibility. Limitations include minor sensitivity variations in highly matrix-loaded or complex environmental samples. Future studies may extend the methodology to simultaneous multi-metal detection and portable, in-field applications. Overall, the proposed method offers a rapid, cost-effective, and highly selective analytical platform for routine environmental monitoring of lead contamination.

Declaration of Competing Interest

The authors declare that they have no known competing financial interests or personal relationships that could have appeared to influence the work reported in this paper.

Funding

The research was supported by Termez State University of Engineering and Agrotechnologies, Termez, Uzbekistan

Acknowledgment

Authors thanks to Termez State University of Engineering and Agrotechnologies, National University of Uzbekistan and Termez branch of Tashkent Medical Academy for support this research work.

References

- Carstea E M, Bridgeman J, Baker A, Reynolds D M, Carstea E M, Bridgeman J, Baker A & Reynolds D M, Fluorescence

- spectroscopy for wastewater monitoring: A review, *Water Res*, **95** (2016) 205–219, doi:10.1016/j.watres.2016.03.021
- 2 Levallois P, Barn P, Valcke M, Gauvin D & Kosatsky T, Public health consequences of lead in drinking water, *Curr Environ Health Rep*, **5** (2018) 255–262, doi:10.1007/s40572-018-0193-0
 - 3 WHO, *Lead in Drinking-Water, Background Document for Development of WHO Guidelines for Drinking water Quality*, World Health Organization, 2011, http://www.who.int/water_sanitation_health/dwq/chemicals/lead.pdf
 - 4 Çubuk S, Salah N, Nallbani B G, Yetimoğlu E K & Kahraman M V, A novel fluorescent chemosensor for sensitive and rapid determination of Pb(II) ions in aqueous environments, *J Fluoresc*, **2024** (2024), doi:10.1007/s10895-024-04034-8.
 - 5 López L, Khan S, Silva M, Gomes Neto J A, Picasso G & Taboada Sotomayor M D P, Systematic study on the synthesis of novel ion-imprinted polymers based on rhodizonate for the highly selective removal of Pb(II), *Reactive Funct Polym*, **159** (2021) 104805, doi:10.1016/j.reactfunctpolym.2020.104805.
 - 6 Özbek O, Kalay E, Berkel C, Aslan O N & Tokalı F S, Synthesis, characterization and sensor properties of a new sulfonyl hydrazone derivative molecule: potentiometric determination of Pb(II) ions, *Chem Pap*, **78** (2024) 2621–2633, doi:10.1007/s11696-023-03267-4
 - 7 Ashirov M A, Yusupova M R, Akhmadjanov U G, Smanova Z A, Khabiyev A, Baigenzhenov O & Berdimurodov E, Sulfarsazen-immobilized PPA matrix as a new efficient analytical reagent for Hg(II) determination, *Adv Biochem Chem Res*, **10** (2023) 135–148, doi:10.22036/abcr.2022.357823.1817.
 - 8 Salami H O, Alahmad W, Darwish I A, Saad Aly M A, Ashfaq M & Kraiya C, Synthesis of poly(acrylic acid) modified graphene/MoS₂ heterostructure-based composite: an effective removal of Pb(II), Cd(II) and Zn(II) from wastewater, *Sci Rep*, **15** (2025) 11701, doi:10.1038/s41598-025-94671-1.
 - 9 Aracier E D, Yetimoğlu E K & Urucu O A, An eco-friendly and sensitive deep eutectic solvent-based liquid-phase microextraction procedure for extraction preconcentration of Pb(II) ions, *Anal Sci*, **39** (2023) 1065–1071, doi:10.1007/s44211-023-00315-7.
 - 10 Topcu C, Yılmaz R R, Atasoy B H, Ocsoy I & Yılmaz V, A novel composite electrochemical sensor doped ion-imprinted polymer based on N-methacryloyl-L-histidine/ethylene glycol dimethacrylate for ultrasensitive determination of copper (II) ions in food supplements, *Chem Pap*, **78** (2024) 8245–8260, doi:10.1007/s11696-024-03664-3.
 - 11 Praveen H & Chandran V G, Impact of doping vanadium pentoxide in poly(O toluidine) on improving electrical conductivity and dielectric characteristics, *J Anal Chem*, **38** (2025) 7, doi:10.1177/08927057251322172.
 - 12 Praveen H & Chandran V G, Investigation on material characterization, dielectric behaviour and electrical conductivity of ZnO-poly(O toluidine) nanocomposites, *Polym Bull*, **82** (2025) 4755–4773, doi:10.1007/s00289-025-05724-4.
 - 13 Kholboyeva M B, Smanova Z A, Madatov U A, Rakhimov S B, Orzikulov B T, Nomozov A K & Uralova M R, Determination of Fe(III) ion with a novel, highly efficient immobilized nitroso R-salt in a polymer matrix, *Chem Rev Lett*, **8** (2025), doi:10.22034/crl.2025.496212.1505.
 - 14 Mansurov D, Khaitbaev A, Khaitbaev K Kh, Toshov K S & Benassi E, Relationship between structural properties and biological activity of (-)-menthol and some menthyl esters, *Comput Biol Chem*, **2025** (2025) doi:10.1016/j.compbiolchem.2025.108357.
 - 15 Khabibullaeva N, Khaitbaev A, Mansurov D, Khakimov Z, Rakhmanov A, Vidovic E & Benassi E, Bioactive composite based on chitosan obtained from the exoskeleton of dead *Apismellifera* and selenium nanoparticles for accelerated skin wound healing: synthesis, characterisation and in vivo assessment, *Int J Biol Macromol*, **2025** (2025), 148334 doi:10.1016/j.ijbiomac.2025.148334.
 - 16 Madusmanova N, Smanova Z, Yakhshieva Z, Yangibayev A, Hudoynazarov I, Yangibayev S, Ahmadjonov O, Gulbakhor K, Babaev B & Benassi E, Determination of Mn(II) ions in soil samples by means of a sensitive sorption spectroscopic method, *Talanta*, **297** (2026) 128770, doi:10.1016/j.talanta.2025.128770.
 - 17 Razzoqova S, Ibragimov A, Torambetov B, Kadirova Sh, Holczbauer T, Ashurov J & Ibragimov B, Synthesis, structure and Hirshfeld surface analysis of a coordination compound of cadmium acetate with 2-aminobenzoxazole, *Acta Crystallogr E Crystallogr Commun*, **79** (2023) 862–866, doi:10.1107/S2056989023007399
 - 18 Ruzmetov U U, Jumaeva E Sh, Orzikulov B T & Smanova Z A, Determination of iron ions in water by flame atomic absorption spectrometry with sorption preconcentration, *Ind Lab Mater*, **89** (2023) 22–30, <https://orcid.org/0000-0002-1498-0236>.
 - 19 Razzoqova S, Torambetov B, Amanova M, Kadirova Sh, Ibragimov A & Ashurov J, Crystallization, structural study and analysis of intermolecular interactions of a 2-aminobenzoxazole-fumaric acid molecular salt, *Acta Crystallogr E Crystallogr Commun*, **78** (2022) 1277–1283, doi:10.1107/S2056989022011185
 - 20 Nazirov Sh S, Turaev Kh Kh, Kasimov Sh A, Tillaev Kh R, Alimnazarov B Sh & Abdullaeva B B, Spectrophotometric determination of Ni(II) ion with 7-bromo-2-nitroso-1-oxinaphthalene-3,6-disulphocid, *Int J Eng Trends Technol*, **72** (2024) 57–63, doi:10.14445/22315381/IJETT-V72I6P106.
 - 21 Bobojonov B, Madatov U, Usmanova X, Smanova Z, Ahmadjonov U, Demir M & Berdimurodov E, Efficient and cost-effective determination of Cr(VI) ions using immobilized 4,5-dihydroxynaphthalene-2,7-disulfonic acid disodium salt dihydrate: A novel analytical reagent with high selectivity and sensitivity, *Int J Environ Anal Chem*, **2023** (2023), doi:10.1080/03067319.2023.2235562.
 - 22 Nomozov A K, Beknazarov Kh, Khodjamkulov S, Misirov Z & Yuldashova S, Synthesis of corrosion inhibitors based on (thio)urea, orthophosphoric acid and formaldehyde and their inhibition efficiency, *Baghdad Sci J*, **22** (2024) 4, doi:10.21123/bsj.2024.10590.
 - 23 Nomozov A, Beknazarov K, Geldiev Y, Babamurodov B E, Muzaffarova N & Yuldashova S G, Synthesis of PFG brand corrosion inhibitor and its quantum chemical calculation results, *Chem Probl*, **23** (2025) 297–309, doi:10.32737/2221-8688-2025-3-297-309.

- 24 Khaitov M B, Abdualimov S, Allanov K, Ikromova M & Ochildiev O, The efficiency of siliciousnano nutrition on cotton productivity in arid regions, *Front Sustain Food Syst*, **8** (2024) 1362369, doi:10.3389/fsufs.2024.1362369.
- 25 Smanova Z, Gafurova D, Savchikov A V, So N NN, So N & Ho N, Disodium 1-(2-pyridylazole)-2-hydroxynaphthalene-3,6-disulfonate: immobilized reagent for iron (III) determination, *Russ J Gen Chem*, **4** (2011) 739–742, doi:10.1134/S1070363211040207.
- 26 Misirov Z, Beknazarov Kh S, Akhmedov U Ch, Nomozov A K & Babamuratov B E, Synthesis and application of corrosion inhibitor for hydrogen sulfide corrosion of steel, *Indian J Chem Technol*, **32** (2023) 101–109, doi:10.56042/ijct.v32i3.7278.
- 27 Nomozov A, Beknazarov K, Normurodov B A, Misirov Z, Yuldashova Kh S G, Mukimova G J, Nabiev D A & Jumaeva Z, Inhibition potential of *Salsola oppositifolia* extract as a green corrosion inhibitor of mild steel in an acidic solution, *Int J Corros Scale Inhib*, **14** (2025) 1103–1115, doi:10.17675/2305-6894-2025-14-3-5.
- 28 Nomozov A K, Beknazarov Kh S, Chorjeva N B, Mirzakulov Kh Ch, Arifdjanova K S, Mukimov A S, Pardaev A A & Ashurova N D, Recent developments in polymer-based composite anticorrosion coatings: Materials, mechanisms and applications, *Int J Corros Scale Inhib*, **14** (2025) 1362–1390, doi:10.17675/2305-6894-2025-14-3-18.
- 29 Nomozov A, Khodjamkulov S, Misirov Z, Umurzakova S, Buranova D, Nurova Z & Soatov S, Antibacterial evaluation, and prediction of the ability of *Salsola oppositifolia* extract, *J Chem Lett*, **6** (2025) 203–211, doi:10.22034/jchemlett.2025.546568.1348.
- 30 Kholmurodova S, Turaev Kh, Alikulov R, Beknazarov K & Eshmurodov E K, Obtaining an organic-inorganic sorbent based on vermiculite modified with urotropin and hydrolyzed polyacrylonitrile, *Chem Rev Lett*, **8** (2025) 267–279, doi:10.22034/crl.2025.481061.1435.
- 31 Nazarov Y E, Turaev Kh Kh, Kasimov Sh A, Ashurov J M, Eshimbetov A G, Ibragimov A B, Nomozov A K, Xia C & Hossain A M S, Synthesis, crystal structures, DFT calculations, and Hirshfeld surface analysis of tris(quinolin-8-olato- κ^2 N,O)cobalt(III) acetic acid monosolvate and bis(μ -quinolin-8-olato- κ^2 N,O)diaquabis(nitrato- κ^2 O,O')dinickel(II) complexes, *J Mol Struct*, **1** (2026) 154569, doi:10.1016/j.molstruc.2026.154569.
- 32 Juraev V, Xakimov K, Khakimova D & Fe₃O₄-ZnO incorporated in chitosan-carbon nanotubes (Fe₃O₄-ZnO-CHIT-CNT) as a hybrid organic inorganic biodegradable nano-composites for application in bone tissue engineering, *J Nanostruct*, **15** (2025) 1380–1393, doi:10.22052/JNS.2025.03.053.
- 33 Allazarov A, Khakimov K & Tursunov C, Study of the influence of tungsten carbide powder granulation on the physical-mechanical properties of the solid alloy, in *AIP Conf Proc*, **3045** (2024) 1.
- 34 Li X & Lin Z, Synthesis of a Pb(II) photoresponsive probe and its application to the rapid determination of Pb(II) in mustard samples, *J Anal Chem*, **80** (2025) 1163–1169, doi:10.1134/S1061934825600349.
- 35 Chen J, Duan Q, Liu J, Zhang S, Zhang J & Lin S, Adsorption of Fe-modified peanut shell biochar for Pb(II) in mixed Pb(II), Cu(II), Ni(II) solutions, *Sci Rep*, **15** (2025) 13558, doi:10.1038/s41598-025-97042-y.
- 36 Omidvar-Motlagh M, Es'haghi Z & Es'haghi Z, Magnetic porous ion imprinted polymer based on surface polymerization and nano-ZnO as sacrificial support for selective extraction and determination of Pb(II) in water samples and cosmetics, *Water Air Soil Pollut*, **235** (2024) 211, doi:10.1007/s11270-024-07013-8.
- 37 Kholmurodova S A, Turaev Kh Kh, Alikulov R, Tashkulov A Kh, Xolnazarov B A & Yuldashova S G, Preparation of vermiculite and polypolyacrylonitrile composite and its modification with diethanolamine, *Chemical Problems*, **1** (2025) 3–19, doi:10.32737/2221-8688-2025-1-3-19.